JB Journals.ASM.org

Streptococcus mutans NADH Oxidase Lies at the Intersection of Overlapping Regulons Controlled by Oxygen and NAD^+ Levels

J. L. Baker,[a] A. M. Derr,[a]* K. Karuppaiah,[b]* M. E. MacGilvray,[b]* J. K. Kajfasz,[b] R. C. Faustoferri,[b] I. Rivera-Ramos,[a] J. P. Bitoun,[c]* J. A. Lemos,[a,b] Z. T. Wen,[c] R. G. Quivey, Jr.[a,b]

Department of Microbiology and Immunology, University of Rochester School of Medicine and Dentistry, Rochester, New York, USA[a]; Center for Oral Biology, University of Rochester School of Medicine and Dentistry, Rochester, New York, USA[b]; Department of Oral and Craniofacial Biology, School of Dentistry, Louisiana State University Health Sciences Center, New Orleans, Louisiana, USA[c]

NADH oxidase (Nox, encoded by *nox*) is a flavin-containing enzyme used by the oral pathogen *Streptococcus mutans* to reduce diatomic oxygen to water while oxidizing NADH to NAD^+. The critical nature of Nox is 2-fold: it serves to regenerate NAD^+, a carbon cycle metabolite, and to reduce intracellular oxygen, preventing formation of destructive reactive oxygen species (ROS). As oxygen and NAD^+ have been shown to modulate the activity of the global transcription factors Spx and Rex, respectively, Nox is potentially poised at a critical junction of two stress regulons. In this study, microarray data showed that either addition of oxygen or loss of *nox* resulted in altered expression of genes involved in energy metabolism and transport and the upregulation of genes encoding ROS-metabolizing enzymes. Loss of *nox* also resulted in upregulation of several genes encoding transcription factors and signaling molecules, including the redox-sensing regulator gene *rex*. Characterization of the *nox* promoter revealed that *nox* was regulated by oxygen, through SpxA, and by Rex. These data suggest a regulatory loop in which the roles of *nox* in reduction of oxygen and regeneration of NAD^+ affect the activity levels of Spx and Rex, respectively, and their regulons, which control several genes, including *nox*, crucial to growth of *S. mutans* under conditions of oxidative stress.

Streptococcus mutans is an oral pathogen that grows on the human tooth surface in dental plaque, a multispecies biofilm environment. Similar to other microbial biofilms, dental plaque contains channels that facilitate fluid movement, delivery of nutrients, and changes in chemical composition (1–3). This structure allows for environmental variations within the biofilm itself, including exposure to differing oxygen concentrations, rapid changes in environmental pH, and large shifts in nutrient availability. *S. mutans* has developed a complex stress response system consisting of intertwining pathways to survive the challenges posed by acute environmental changes experienced in the oral cavity (4–6).

Two of the major environmental stresses to which the organism must adapt in the oral cavity are acid exposure and oxidative stress. *S. mutans* has evolved several mechanisms to respond to acid stress, including upregulation of F-ATPase activity (7, 8), reduced phosphotransferase activity (9, 10), cytosolic alkalinization through the use of the agmatine deiminase system (5, 11) or malolactic fermentation (12), and alteration of membrane fatty acid composition (13, 14). In addition to acid stress, *S. mutans* must also cope with exposure to oxidative stress, created by diatomic environmental oxygen present in the oral cavity, as well as copious amounts of H_2O_2 produced by competing oral microflora in an attempt to thwart persistence and proliferation of *S. mutans* and other cariogenic bacteria (15–19). *S. mutans* encodes several enzymes important in eliminating potentially dangerous reactive oxygen species (ROS) (20). The *nox* gene (SMU.1117) encodes the flavin-based NAD (NADH) oxidase (Nox), which acts to reduce oxygen, one electron at a time, to H_2O, through the oxidation of NADH to NAD^+ (21, 22). Our laboratory has previously shown that Nox is the major oxygen-metabolizing enzyme used by *S. mutans*, responsible for reduction of approximately 40% of the dissolved oxygen encountered in dental plaque, and that the Nox enzyme shows elevated activity under conditions of both oxidative stress and low pH (21). Mutation of *nox* in the genomic type strain, *S. mutans* UA159, has demonstrated that NADH oxidase plays a role in the acid stress response, as inactivation of *nox* invokes changes in membrane fatty acid composition and metabolic output reminiscent of those seen during exposure to low pH (21, 23–25). In addition to reducing oxygen, Nox is also critical in the regeneration of NAD^+, a key molecule in the production of pyruvate during carbon metabolism in streptococci (26–29). The contributions of the Nox enzyme to the acid and oxygen stress responses, as well as metabolism, are extremely important to *S. mutans*, an organism that lacks catalase, cytochrome oxidases, and an electron transport system (30).

Two proteins that have been implicated in *nox* regulation are the transcription factors Spx, the suppressor of ClpP and ClpX, and Rex, the redox-sensing regulator (21, 31, 32). The Spx regulator senses the redox state through a CXXC motif and has been described previously in many firmicutes, including *Bacillus subtilis* (33–36). Two homologs of Spx, SpxA (SMU.1142) and SpxB (SMU.2084), have been described in *S. mutans* (32, 37). Mounting evidence suggests that both proteins are able to positively regulate

Received 7 February 2014 Accepted 25 March 2014
Published ahead of print 28 March 2014
Address correspondence to R. G. Quivey, Jr., Robert_Quivey@urmc.rochester.edu.
* Present address: A. M. Derr, Food and Drug Administration, Rockville, Maryland, USA; K. Karuppaiah, Department of Developmental Biology, Washington University School of Medicine, St. Louis, Missouri, USA; M. E. MacGilvray, Laboratory of Genetics, University of Wisconsin—Madison, Madison, Wisconsin, USA; J. P. Bitoun, Department of Microbiology and Immunology, Tulane University School of Medicine, New Orleans, Louisiana, USA.
A.M.D. and J.L.B. contributed equally to this work.

doi:10.1128/JB.01542-14

TABLE 1 Strains used in this study

Strain	Description	Source or reference
S. mutans		
UA159	Genomic type strain	20, 44
JL12	*spxA* mutant strain	37
JL13	*spxB* mutant strain	37
JL21	*spxAB* double-mutant strain	32
UR130	UA159 transformed with pBGKnox119CAT	
UR250	JL13 transformed with pBGKnox119CAT	
UR251	JL12 transformed with pBGKnox119CAT	
UR252	JL21 transformed with pBGKnox119CAT	
MU1020	*nox* deletion strain (Δ*nox*)	
MU0961	*rex* deletion strain (Δ*rex*)	
UR281	UA159 transformed with pBGKnox516CAT	
UR322	Δ*rex* transformed with pBGKnox119CAT	
UR323	Δ*rex* transformed with pBGKnox516CAT	
E. coli		
DH10B	Host for cloning vector	Invitrogen
Rosetta	Host for expression vector (SpxB)	Novagen
M15	Host for expression vector (Rex)	Qiagen
DH5α	Host for expression vector (SpxA)	Invitrogen

genes encoding oxygen stress response enzymes, although SpxB appears to play a secondary role in this regulation (21, 32). In addition to Spx, the Rex regulatory protein (SMU.1053) has been implicated in the repression of energy metabolism, maintenance of oxygen homeostasis, and biofilm formation in response to changes in the redox potential of *S. mutans* and several other species of Gram-positive bacteria (31, 38–41). Rex senses the redox state by binding to the cofactor NAD^+ or NADH, which enhance or inhibit the binding of Rex to target promoters, respectively (38, 40–43).

In this study, the effects of addition of exogenous oxygen or deletion of *nox* on global transcription in continuous cultures of *S. mutans* were characterized using cDNA microarray analysis. Several important trends were observed in both cases, including altered expression of genes involved in oxidative stress, energy metabolism, and transport. Several transcription factor-encoding genes, including *rex*, were upregulated in the Δ*nox* mutant only. The promoter region of *nox* was characterized, and regulatory partners were identified in an attempt to further understand the governance of *nox* and the oxygen response. Oxygen, as well as SpxA and Rex, positively influenced *nox* transcription. Since *nox* controls the levels of oxygen and NAD^+, cofactors of SpxA and Rex, respectively, the data presented below place *nox* in the center of a regulatory loop with the SpxA and Rex regulons as downstream effectors.

MATERIALS AND METHODS

Bacterial strains and growth conditions. All *S. mutans* strains listed in Table 1 are derivatives of the genomic type strain, *S. mutans* UA159 (44), and were maintained on brain heart infusion (BHI) (BD/Difco, Franklin Lakes, NJ) agar at 37°C in a 5% (vol/vol) CO_2-95% air environment. Antibiotics were added to a final concentration of 5 μg ml^{-1} for erythromycin and 1 mg ml^{-1} for kanamycin. Organisms were cultured in TY medium (3% tryptone, 0.1% yeast extract, 0.5% KOH, 1 mM H_3PO_4) plus 1% (wt/vol) glucose and were grown in liquid culture or in continuous culture in a BioFlo 2000 fermentor (New Brunswick Scientific, Edison, NJ) as described previously (13, 45). Continuous cultures were grown at a dilution rate of 0.24 h^{-1} under glucose-limiting conditions (2.3 mM), with a continuous impeller speed of 200 rpm, unless otherwise indicated. Steady-state pH levels of 7.0 or 5.0 were maintained by the addition of 2 N KOH. The oxygen concentration was controlled by addition of air to the fermentor vessel at a rate of 1 vessel volume min^{-1} (VVM), and the impeller speed was automatically adjusted to regulate oxygen diffusion on demand. The culture pH and dissolved-oxygen (DO) concentration were continuously monitored throughout the experiment by using an indwelling pH probe (Mettler Toledo, Columbus, OH) and an InPro 6000 oxygen sensor electrode (Mettler Toledo, Columbus, OH), respectively. After a continuous culture had been maintained for a minimum of 10 generations under a given condition, aliquots of the culture were removed and cells were collected by centrifugation. Cell pellets were washed and stored frozen at −80°C. Batch cultures in which the oxygen concentration was controlled were grown in a fermentor vessel at 37°C to an optical density at 600 nm (OD_{600}) of 0.5, and the oxygen concentration was monitored and controlled as described for continuous cultures.

Escherichia coli was grown on LB agar medium at 37°C. Liquid cultures were grown with shaking at 37°C. Antibiotics were added to a final concentration of 50 μg ml^{-1} for kanamycin, 500 μg ml^{-1} for erythromycin, and 20 μg ml^{-1} for chloramphenicol.

DNA manipulations. Chromosomal DNA was isolated from *S. mutans* as previously described (46). Plasmid DNA was isolated from *E. coli* as previously described using a Qiagen mini-prep kit (Qiagen, Chatsworth, CA) or an E.Z.N.A Plasmid minikit (Omega Bio-Tek, Norcross, GA). PCR was carried out with Platinum *Taq* DNA polymerase (Invitrogen, Carlsbad, CA). Amplicons were isolated and purified via gel electrophoresis as previously described (7). *S. mutans* UA159 was transformed by previously described methods (44, 47).

Generation of recombinant *S. mutans* strains. The entire coding region of *nox* (SMU.1117) or *rex* (SMU.1053) was deleted from mutant strains of *S. mutans* UA159 using a PCR-based, ligation-independent cloning method (LIC mutagenesis) described previously (48–50). Briefly, approximately 400 bp upstream and downstream of the gene of interest was used to mediate recombination of the construct into genomic DNA at the appropriate position. The generation of strains with *spxA*, *spxB*, or both deleted has been described previously (37). The deletion strains are listed in Table 1. Appropriate constructs were verified using specific primers for each strain (Table 2).

To create *nox*-chloramphenicol acetyltransferase (CAT) reporter fusions, the intergenic sequence directly upstream of SMU.1117 was amplified using primers detailed in Table 2 to produce constructs containing varying lengths of the promoter region. Primers 119noxFor and 516noxRev (Table 2) were used to amplify 516 bp of the proposed promoter region. The proximal 119 bp of the *nox* promoter region was amplified using the primer pair 119noxFor and 119noxRev (Table 2). The amplified products were gel purified, digested with appropriate restriction enzymes, and cloned into similarly digested pENTR-CAT (21). Subsequently, pENTR-CAT containing either the 516-bp or 119-bp intergenic region preceding SMU.1117 was digested with XmnI and EcoRV and subcloned into the SmaI site of the streptococcal integration vector pBGK (51). The recombinant plasmids were named pBGKnox516CAT and pBGKnox119CAT, respectively (Table 3). Plasmid pBGKnox516CAT was used to transform *S. mutans* UA159 and *S. mutans* MU0961 (Δ*rex*), with selection for kanamycin resistance. The resulting colonies were screened by PCR to verify the integration of constructs into the chromosome. Strains containing the *nox* promoter fragment in the *gtfA* locus were designated UR281 (UA159 background) and UR323 (Δ*rex* background) (Table 1). Plasmid pBGKnox119CAT was transformed into *S. mutans* strains UA159, JL13 (Δ*spxA*), JL12 (Δ*spxB*), JL21 (Δ*spxAB*), and MU0961 (Δ*rex*) (32, 37) (Table 1), and transformants were selected on BHI agar containing kanamycin. The transformants were verified by PCR, and the strains were designated UR130 (UA159 background), UR251 (Δ*spxA* background), UR250 (Δ*spxB* background), UR252 (Δ*spxAB* background), and UR322 (Δ*rex* background) (Table 1).

TABLE 2 Primers used in this study

Primer name	Sequence (5′–3′)	Application
119*nox*Rev	GGCGGCGGATCCCCATTTTGGAGATTATAAA	119-bp CAT-promoter construct
119*nox*For	GGCGGCGCGGCCGCAAGCAAATCCTCTTTT	119- and 516-bp CAT-promoter construct; EMSA
516*nox*Rev	GGCGGCGGATCCCTTTGCAGGAACGACCAT	516-bp CAT-promoter construct; EMSA
*nox*pe-F1	CAACTTCGTTTTCACTACCG	Primer extension, sequencing
trxA RTF	TTGAAGCTGAAACGGCTAAGGG	qRT-PCR of *trxA*
trxA RTR	GCCTGCATAAGACATGGACCAC	qRT-PCR of *trxA*
trxB RTF	AGTTGTTGGTGGTGGCGATTC	qRT-PCR of *trxB*
trxB RTR	CATTGGCAAAGGCACGTTCTTG	qRT-PCR of *trxB*
tpx RTF	CTCCATCTGCTTGGACGTGCTG	qRT-PCR of *tpx*
tpx RTR	GCAAGGGCAGCGTCATAGTTG	qRT-PCR of *tpx*
gor RTF	ACCTGTGTTAATGTTGGCTGTG	qRT-PCR of *gor*
gor RTR	CCTGACGATTTTGCTTCAAGAC	qRT-PCR of *gor*
sod RTF	AGCACTTGATGTCTGGGAACAC	qRT-PCR of *sod*
sod RTR	CGGCATAAAGACGAGCAACAG	qRT-PCR of *sod*
dpr RTF	GAAGAAACAGTTGGCACATGGG	qRT-PCR of *dpr*
dpr RTR	TTCCGTTTGAGCTGCTGTAAAG	qRT-PCR of *dpr*
ahpC RTF	ATGGTTTAGCACAACGTGGAAC	qRT-PCR of *ahpC*
ahpC RTR	TTGGCAGGGCAAACTTCTCC	qRT-PCR of *ahpC*
ahpF RTF	GCGTCCGCCTAAGGTAGAG	qRT-PCR of *ahpF*
ahpF RTR	TGAAAGCCTGAACAACATCTGG	qRT-PCR of *ahpF*
rex RTF	ATAGCGGAAGCCATTGGTATCG	qRT-PCR of *rex*
rex RTR	ATTGCCAACTCCCACAAGAAGG	qRT-PCR of *rex*
5′ IVT *nox*	GAATAGTATTAATGGCAGGC	*In vitro* transcription of *nox*
3′ IVT *nox*	GTAGAGAAGTCCATTTTGGA	*In vitro* transcription of *nox*
5′ *spxA* pMal EcoRI	AAGGGGTAGTGAATTCATGGTTACC	Cloning of SpxA coding region
3′ *spxA* pMal BamHI	GGGTAAGCGGAATTCTTAGTCATCTTC	Cloning of SpxA coding region
5′ *spxB* pMal BamHI	TGAGCTTGAAGAGGATCCAAAAATAGGTCC	Cloning of SpxB coding region
3′ *spxB* pMal EcoRI	TCATTACTTCGAGAATTCTTATAAAGCTGC	Cloning of SpxB coding region
Δ*rex*F	ACTCCAGATGAGGTTAAGGC	Construction of *rex* deletion mutant
Δ*rex*R	CAAGCGAGAATGACCTGCG	Construction of *rex* deletion mutant
MU1020P7UP	AAGTTGAGGTATTAGAGATAGGTCG	Construction of *nox* deletion mutant
MU1020P8DN	TTGATGCGTTATCTCGGTG	Construction of *nox* deletion mutant

Chloramphenicol acetyltransferase activity assay. Chloramphenicol acetyltransferase assays for the measurement of transcriptional regulation were performed according to the method of Kuhnert et al. (52, 53). Briefly, 50-ml cell pellets were resuspended in 1 ml 10 mM Tris-Cl, pH 7.8. The cells were lysed using 0.1-mm glass beads in a Mini-Bead Beater (BioSpec Products, Bartlesville, OK). Cell debris was removed by centrifugation at 10,000 rpm for 10 min. The lysates were removed and used for total-protein quantification and CAT assays. Each CAT assay reaction mixture consisted of 50 μl whole-cell lysate, 100 mM Tris-Cl, pH 7.8, 0.1 mM acetyl-coenzyme A (acetyl-CoA), and 0.4 mg ml^{-1} 5,5′-dithio-bis(2-nitrobenzoic acid) (DTNB) in a total volume of 1 ml. Reactions were initiated by addition of 0.1 mM chloramphenicol. Optical density measurements at 412 nm were monitored over 3 min. The reaction rate and total-protein concentration were used to determine CAT activity. Results are given in nmol of chloramphenicol acetylated min^{-1} mg total $protein^{-1}$.

TABLE 3 Plasmids used in this study

Plasmid	Description
pBGK	Streptococcal integration vector (51)
pENTRCAT	pENTR4 (Invitrogen) containing promoterless CAT (Promega) (21)
pBGKnox516CAT	pBGK derivative containing the 516-bp *nox* promoter in front of CAT
pBGKnox119CAT	pBGK derivative containing the 119-bp *nox* promoter in front of CAT
pBRnox	Template for sequencing ladder (21)
pMALc2X	Protein expression vector (SpxA and SpxB) (New England Biolabs)
pQE30	Protein expression vector (Rex) (Qiagen)
pQE-*rex*	pQE30 containing *rex* (38)

cDNA microarray analysis. *S. mutans* UA159 microarray slides were provided by the J. Craig Venter Institute (JCVI) through a cooperative agreement with the National Institutes for Allergy and Infectious Disease (NIAID) and Dental and Craniofacial Research (NIDCR). Reference RNA was isolated from UA159 cells grown in BHI medium to an optical density at 600 nm of 0.5 and purified as previously described (9). *S. mutans* UA159, grown with or without 8.4% exogenous oxygen, or the Δ*nox* strain was grown to a steady-state pH value of 7, with four replicate cultures of each. Total RNA was isolated and purified as previously described (9, 32). cDNA was synthesized and labeled using Cy3-dUTP or Cy5-dUTP (GE Healthcare, Piscataway, NJ) as previously outlined (9). Cy3-dUTP-labeled test cDNA and Cy5-dUTP-labeled reference cDNA were hybridized overnight at 42°C. Hybridization was carried out using a Maui Hybridization system (BioMicro Systems, Inc., Salt Lake City, UT), washed according to protocols provided by JCVI, and scanned using a GenePix 4000b Microarray Scanner (Molecular Devices, Inc., Sunnyvale, CA). After scanning, the images were analyzed using TIGR Spotfinder and normalized, as previously described (9). Statistical analysis was carried out using BRB array tools (http://linus.nci.nih.gov/BRB-ArrayTools.html).

Real-time quantitative RT-PCR. Real-time quantitative reverse transcription-PCR (qRT-PCR) was performed as described previously (9, 32) using a StepOnePlus real-time PCR system (Applied Biosystems, Carlsbad, CA). Gene-specific primers were designed using Beacon Designer 4.0

software (Premier Biosoft International, Palo Alto, CA) and are listed in Table 2. RNA was isolated from UA159 grown either to steady state in the chemostat at pH values of 7 and 5 or in batch cultures in TY medium plus 1% (wt/vol) glucose titrated to pH 7 or 5. The mRNA copy number was quantified based on a standard curve of PCR product, as previously described (54). Student's *t* test was performed to determine the significance of the PCR quantifications.

Primer extension assay. Total-RNA samples were extracted from cultures of *S. mutans* UA159 grown to steady state at a pH value of 5 or 7 under controlled oxygen conditions, as previously described (21, 55). RNA isolation was performed as outlined above (7). Primer extension analysis of 50 μg total RNA was performed using the Promega AMV Reverse Transcriptase Primer Extension System (Promega, Madison, WI). The primer *nox*pe-F1 (Table 2) (10 pmol) was end labeled with [γ-^{32}P]ATP (6,000 Ci/mmol; PerkinElmer, Boston, MA) and T4 polynucleotide kinase (PNK) (Life Technologies, Carlsbad, CA). The primer extension products were separated on an 8% denaturing acrylamide gel alongside a sequencing ladder created with pBRnox DNA and *nox*pe-F1 using the Sequenase v2.0 sequencing kit (USB Biochemicals, Cleveland, OH).

Spx protein production. SpxA and SpxB from *S. mutans* were produced as recombinant proteins fused to a maltose-binding protein tag in pMALc2X (New England BioLabs, Ipswitch, MA). Both SpxA (SMU.1042) and SpxB (SMU.2084) were cloned into pMALc2x, using BamHI and EcoRI restriction sites. Protein expression was induced by growing *E. coli* DH5α (for SpxA) or Rosetta (for SpxB) by inoculating 1 liter LB plus 1% (wt/vol) glucose (1:100) with an overnight culture grown in LB medium. The resulting culture was grown at 37°C with shaking (200 rpm) until an OD_{600} of 0.5 was reached, at which point the cultures were transferred to 15°C, and 0.3 mM isopropyl β-D-1-thiogalactopyranoside (IPTG) was added to induce production of the tagged protein overnight. Pellets were collected by centrifugation and then resuspended in column buffer (20 mM Tris-HCl, 200 mM NaCl, 1 mM EDTA). The cells were subjected to 3 30-s cycles of homogenization in a Mini Bead Beater (BioSpec Products, Bartlesville, OK) with chilling on ice between cycles. After centrifugation, purification of the recombinant proteins was performed by column chromatography using amylose resin (New England BioLabs, Ipswitch, MA). Recombinant SpxA and SpxB were eluted in column buffer containing 10 mM maltose. Protein concentrations were determined using the bicinchoninic acid (BCA) assay (Sigma, St. Louis, MO) (56).

***In vitro* transcription of *nox*.** A linear *nox* promoter DNA template was generated by PCR using primers 5′IVT *nox* and 3′IVT *nox* (Table 2) to yield a 191-bp nucleotide fragment that would direct the synthesis of an approximately 62-bp nucleotide transcript. The *in vitro* transcription (IVT) reaction was performed as described by Lin and Zuber (57). Briefly, 10 nM *nox* promoter template, 25 nM *B. subtilis* RNA polymerase (RNAP), and 25 nM *B. subtilis* σ^A or RpoA were incubated with or without 375 nM SpxA or SpxB protein and with or without 5 mM dithiothreitol (DTT) in 10 mM Tris-HCl, pH 8.0, 50 mM NaCl, 5 mM $MgCl_2$, and bovine serum albumin (BSA) (50 μg ml^{-1}) for 10 min at 37°C. A nucleotide mixture (200 mM [each] ATP, GTP, and CTP; 10 mM UTP; 5 μCi [α-^{32}P]UTP) was added, and the incubation proceeded for an additional 3 min. Stop solution (1 M ammonium acetate, 0.1 mg ml^{-1} yeast RNA, 0.03 M EDTA) was added, and the mixture was precipitated with ethanol at 4°C overnight. The nucleotide pellet was dissolved in formamide dye (0.3% xylene cyanol, 0.3% bromophenol blue, 12 mM EDTA dissolved in formamide). The samples were heated at 90°C for 2 min and then placed on ice before being applied to an 8% polyacrylamide-urea gel. The transcripts were visualized by autoradiography after overnight exposure to Kodak BioMax MS film (Carestream Health, Inc., Rochester, NY). *B. subtilis* RNAP and σ^A were kind gifts from Peter Zuber, Oregon Health and Science University, Beaverton, OR.

Overexpression and purification of Rex. The expression and purification of Rex have been described previously (38). Briefly, the *rex* coding sequence was PCR amplified and directly cloned into pQE30 (Qiagen, Inc., Valencia, CA) following the manufacturer's instructions. *E. coli* DH10B (Invitrogen, Carlsbad, CA) was used for plasmid amplification, and the insert was confirmed by DNA sequencing. The plasmid pQE-*rex* was transformed into the host *E. coli* M15 (Qiagen, Inc.). The recombinant N-terminal His-tagged Rex protein (rRex) was expressed by IPTG (0.2 mM) induction and purified using an Ni-nitrilotriacetic acid (NTA) column (Qiagen, Inc.) according to the manufacturer's instructions. The purified rRex was washed extensively with 20 mM Tris, pH 7.6, 250 mM NaCl; concentrated; and desalted. The concentration of Rex was determined using the extinction coefficient 10.32 mM^{-1} cm^{-1}.

EMSA. Electrophoretic mobility shift assays (EMSAs) were performed as previously described (38). Briefly, a DNA fragment containing 516 bp of the *nox* promoter region was amplified by PCR using primers shown in Table 2. DNA products were gel purified and end labeled with T4 PNK and [γ-^{32}P]ATP (PerkinElmer, Waltham, MA) for 10 min at 37°C. Quantification of the labeled DNA was performed by scintillation counting. A representative binding reaction mixture (20 μl) consisted of the following: binding buffer (20 mM Tris, pH 8.0, 1 mM EDTA, 75 mM KCl, 0.5 mM DTT, 10% glycerol), radiolabeled DNA probe (5,000 cpm), and purified Rex. The reaction mixture was incubated at room temperature for 10 min. When 10 mM NAD^+ or NADH was included in the reaction mixture, the samples were incubated for an additional 15 min upon the addition of NAD^+ or NADH. Rex-DNA binding was assessed using a 5% nondenaturing polyacrylamide gel in 1× Tris-borate-EDTA (TBE) buffer. The gels were exposed to a phosphorimager screen, and binding was detected with a Molecular FX phosphorimager and Bio-Rad Quantity One software (Bio-Rad, Hercules, CA).

Microarray data accession number. The microarray data have been deposited in the NCBI Gene Expression Omnibus (GEO) database (http://www.ncbi.nlm.nih.gov/geo) with accession number GSE38803.

RESULTS

Addition of dissolved oxygen or loss of *nox* results in global effects on transcription in *S. mutans*. It has been shown previously that a *nox* deletion mutant (Δ*nox*) of *S. mutans* has decreased ability to metabolize oxygen, leading to an increase in the dissolved-oxygen concentration of the culture (8.4% O_2) compared to the dissolved-oxygen concentration in the parental strain, UA159, grown under similar conditions upon reaching steady state (<1% O_2) (21). It is unclear whether differences observed between the Δ*nox* strain and UA159 are directly due to the elevated oxygen concentration experienced by the Δ*nox* strain or due to the loss of Nox functions other than oxygen reduction (such as regeneration of NAD^+). Previously, changes in global transcription of *S. mutans* in response to acidic and oxygen stresses had been analyzed in cultures grown to exponential growth phase (58–60). Here, the tightly controlled environment of the chemostat was used to generate samples in which the external variables, such as nutrients, pH, and oxygen levels, could be rigorously regulated and adjusted. Therefore, to determine any effects of the loss of *nox* distinct from the effects of the resulting elevated oxygen concentration, two sets of comparisons were made.

First, to elucidate the oxygen stress regulon in UA159, cultures were grown to steady-state pH values of 7 while maintaining an oxygen concentration of 8.4% via addition of air to the culture and measured by an indwelling dissolved-oxygen probe to mimic the oxygen stress seen in the Δ*nox* mutant strain (21). These cultures were compared by microarray and qRT-PCR to UA159 cultures grown similarly but without addition of exogenous oxygen (thus, the initial oxygen in the culture was metabolized, and an oxygen concentration of <1% was achieved upon reaching steady state). At an assigned *P* value of 0.05 and a 1.5-fold cutoff, 140 genes were upregulated and 88 genes were downregulated in cultures grown

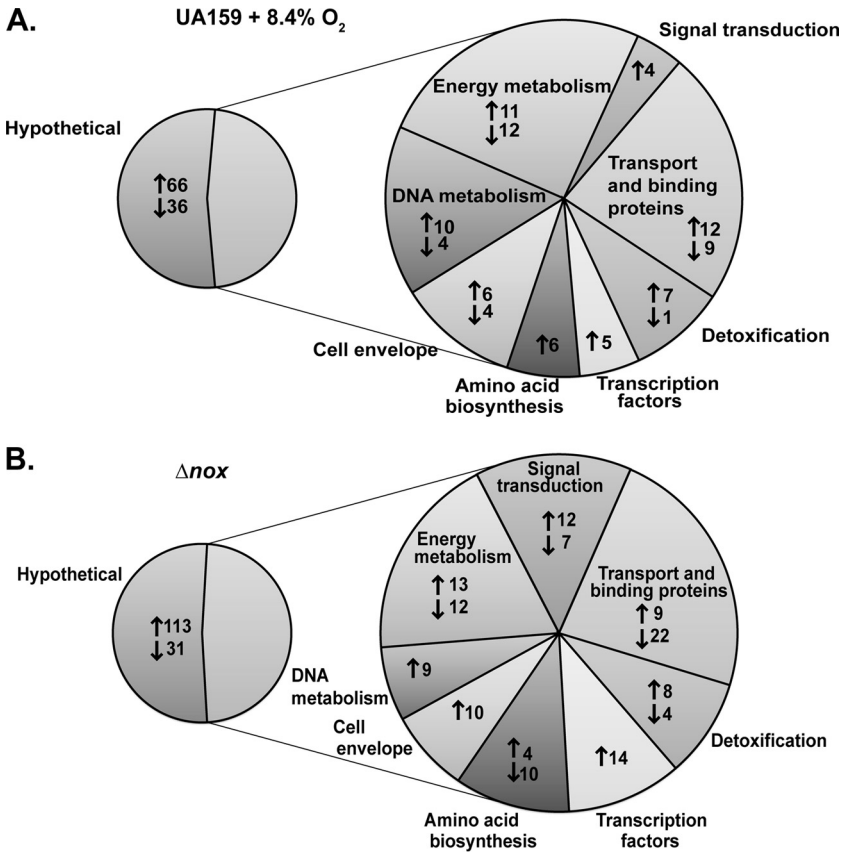

FIG 1 Overview of microarray analysis. The pie charts show overrepresented functional categories with altered expression in UA159 plus 8.4% O_2 compared to UA159 grown without added O_2 (A) and the Δ*nox* strain compared to UA159 grown without added O_2 (B). The numbers next to the up arrows indicate the numbers of genes upregulated, and those next to the down arrows indicate the numbers of genes downregulated. Genes encoding hypothetical proteins were separated out to allow better visualization of genes with known functions.

in 8.4% oxygen compared to cultures grown without exogenous oxygen (data not shown). As shown in Fig. 1, genes involved in energy metabolism, transport, DNA metabolism, and detoxification and encoding hypothetical proteins made up a large portion of the genes exhibiting altered expression in the microarray data. In addition to the microarray analysis, qRT-PCR was performed on several genes of interest to provide more sensitive, quantitative data and to validate shifts seen in the microarray. As expected, upregulation of genes associated with the oxygen stress response was observed; for example, microarray data showed increased transcription of *trxB*, *tpx*, *gor*, *dpr*, and *ahpF*, while qRT-PCR showed increased transcription of *tpx*, *gor*, *sod*, and *ahpC* (Table 4). As *S. mutans* relies strictly on fermentation pathways to generate energy, it was expected that genes producing sugar fermentation pathway enzymes would be differentially expressed with increases in the oxygen concentration (28–30, 61, 62). This was indeed the case, as demonstrated by the microarray analysis showing an increase in transcription of the acetoin dehydrogenase genes *adhABCD* and the pyruvate formate-lyase gene, *pfl* (Table 5). *S. mutans* encodes only a partial tricarboxylic acid (TCA) cycle, and of those genes, *citB*, *citC*, and *citZ* were all downregulated in microarray analysis (Table 5). Lastly, the competence-specific two-component system response regulator *comE* was also upregulated (Table 5).

The second comparison was made to address the possibility that the loss of *nox* may result in additional effects independent of the increased dissolved-oxygen concentration experienced by the Δ*nox* strain. RNA was extracted from the Δ*nox* strain grown to steady state at a pH value of 7 and compared by microarray and

TABLE 4 Expression ratios of genes involved in detoxification of oxidative stress

Gene name	Description	Expression[a]			
		UA159 + 8.4% O_2		Δ*nox*	
		Array	qRT-PCR	Array	qRT-PCR
trxA	Thioredoxin	ND	1.1[d]	3.5[b]	4.0[d]
trxB	Thioredoxin reductase	2.6[b]	NA	ND	NA
tpx	Thiol peroxidase	4.7[b]	6.0[d]	4.1[b]	4.3[d]
gor	Glutathione oxidoreductase	1.9[b]	3.0[d]	1.6[b]	3.6[d]
sod	Superoxide dismutase	ND	1.8[d]	2.1[b]	1.9[d]
dpr	Peroxide resistance protein	2.3[c]	NA	2.7[c]	NA
ahpC	Alkyl hydroperoxide reductase	ND	1.8[d]	3.1[c]	3.6[d]
ahpF	NADH oxidase (H_2O_2 forming)	1.7[b]	NA	2.5[c]	NA

[a] Array data are relative levels of expression compared to expression in *S. mutans* UA159. qRT-PCR data are gene copy numbers relative to those observed in *S. mutans* UA159. ND, no significant differences in expression were detected by microarray analysis; NA, not attempted.
[b] $P \leq 0.05$.
[c] $P \leq 0.01$.
[d] $P \leq 0.0001$.

TABLE 5 Expression ratios of selected genes identified by microarray analysis

Gene name	Function[a]	Expression[b]	
		UA159 + 8.4% O_2	Δ*nox*
adhA	Acetoin dehydrogenase, α subunit	2.8[c]	1.4[d]
adhB	Acetoin dehydrogenase, β subunit	3.6[c]	ND
adhC	DHLA acetyltransferase	5.0[c]	1.5[d]
adhD	DHLA dehydrogenase	3.26[c]	ND
citZ	Citrate synthase	0.37[c]	ND
citB	Aconitate hydratase aconitase	0.42[d]	ND
citC	Isocitrate dehydrogenase	0.32[c]	ND
ldh	Lactate dehydrogenase	ND	1.5[d]
pfl	Pyruvate formate-lyase	1.6[d]	1.9[c]
comD	HK of competence regulon	ND	3.0[d]
comE	RR of competence regulon	5.0[c]	3.2[d]
comYA	Competence ABC transporter	ND	2.5[d]
rex	Redox-sensing repressor	ND	2.4[d]
mutY	DNA glycosylase	ND	3.2[d]

[a] DHLA, dihydrolipoamide; HK, histidine kinase; RR, response regulator.
[b] Relative levels of expression compared to expression in *S. mutans* UA159. ND, no significant differences in expression were detected by microarray analysis.
[c] $P \leq 0.01$.
[d] $P \leq 0.05$.

qRT-PCR (oxidative-stress genes) to UA159 cultures grown to steady state at pH 7 without addition of oxygen. The number of genes differentially expressed in the Δ*nox* strain compared to UA159 grown without addition of exogenous oxygen was greater than the number of genes differentially expressed in UA159 grown with addition of exogenous oxygen compared to UA159 grown without addition of exogenous oxygen. Compared to UA159, microarray data revealed that 220 genes were upregulated in the Δ*nox* strain and 107 genes were downregulated. Once again, genes with altered expression were involved in energy metabolism, transport, DNA metabolism, and detoxification, with hypothetical proteins representing the most abundant category in the microarray data. Additionally, genes involved in signal transduction and encoding transcription factors were overrepresented to a greater extent in the Δ*nox* strain microarrays than in the UA159-plus-8.4% oxygen microarrays, likely resulting from effects of the loss of *nox* independent of the increased dissolved-oxygen level (Fig. 1). Similar to results obtained using RNA from UA159 grown with 8.4% oxygen, the Δ*nox* mutant strain microarray and qRT-PCR analysis demonstrated upregulation of the oxygen stress genes *sod*, *gor*, and *tpx*; in addition, *trxA* was upregulated and the H_2O_2-forming NADH oxidase and NADH peroxidase genes, *ahpC* and *ahpF*, were upregulated to a greater extent than in UA159 grown under 8.4% oxygen conditions (Table 4). Several genes encoding competence cascade proteins were again upregulated, with elevated transcription of *comD*, *comE*, and *comYA* (Table 5). We previously reported that the gene encoding the DNA glycosylase enzyme MutY exhibits elevated transcript levels in a Δ*nox* mutant strain (21), which was verified here, as *mutY* was upregulated in microarray data from the Δ*nox* mutant strain (Table 5). Genes involved in the sugar fermentation pathway were also affected, with transcription of *pfl*, the lactate dehydrogenase gene (*ldh*), and the lactose repressor gene *lacR* exhibiting upregulation, while the majority of the *lac* operon was downregulated (Table 5 and data not shown). Significantly, the global repressor Rex was upregulated more than 2-fold in the Δ*nox* mutant but does not appear to be differentially regulated in the parental strain during growth under elevated oxygen conditions (Table 5). The transcriptional changes seen in the Δ*nox* mutant exhibit many similarities to transcriptional changes seen upon addition of exogenous oxygen, as one would expect from the higher dissolved-oxygen concentration due to impaired ability by the mutant to reduce oxygen. Yet, as we indicated above, there were transcriptional differences observed in the absence of *nox* that are not seen upon addition of exogenous oxygen.

Regulation of *nox* by oxygen occurs within a 119-bp region of the gene promoter. As *nox* clearly plays a role in the oxidative-stress response in *S. mutans*, the *nox* promoter was characterized to uncover how the expression of *nox* is governed. Primer extension analysis identified a guanine nucleotide, located 37 bp from the *nox* translational start site, as the transcriptional start site for the *nox* gene (Fig. 2A). We examined the architecture of the *nox* promoter and identified putative RNA polymerase-binding −10 and −35 consensus regions, as well as the ribosome-binding site (RBS), at expected locations (Fig. 2C). The results from primer extension experiments also indicated that transcription of *nox* was elevated when UA159 was grown in the presence of 8.4% oxygen at pH 7 compared to growth at pH 7 without addition of oxygen (Fig. 2A). qRT-PCR confirmed the increase in *nox* transcription when grown with the addition of oxygen (Fig. 2B). qRT-PCR also showed that in the presence of oxygen, *nox* transcription was elevated even further at pH 5 (Fig. 2B). This finding further supports previous work that showed elevated NADH oxidase activity at low pH (21). Although not further developed in the present study, additional experiments are under way to examine the global synergistic effects of low pH and oxidative stress, through addition of oxygen or deletion of *nox*, on the *S. mutans* transcriptome.

Previous reports have suggested that *nox* transcription is positively regulated by the RNA polymerase-binding proteins SpxA and SpxB and by the DNA-binding protein Rex (31, 32, 38). A fuzznuc algorithm (63) was used to identify a putative Spx regulatory binding motif, $AGCAW_{11}AGCG$, in the −30 region (Fig. 2C), resembling an established Spx motif ($AGCAW_{12}AGCG$) described in the *trxB* promoter region of *B. subtilis* (64). Recent reports of studies with *S. mutans* describing Rex, a regulator involved in redox sensing, have shown that *nox* expression is downregulated in a *rex* mutant, suggesting that the *nox* gene may also be regulated by Rex (31, 38). Fuzznuc (63) also identified two putative Rex motifs, WWRYDWDVHHHWWHDHWW (38), upstream of the *nox* start site: the first was located 202 bp upstream of the transcriptional start site, and the second was located 54 bp upstream of the transcriptional start site (Fig. 2C). These findings strongly suggest that Spx and Rex directly regulate *nox* transcription.

To determine the promoter length required for transcriptional control of NADH oxidase by oxygen, two CAT reporter fusions were created containing either 119 or 516 bp directly upstream of the *nox* gene. Batch cultures of the two *nox* promoter CAT fusion-containing strains were grown in a fermentor equipped with an oxygen probe and harvested at mid-log phase, with or without addition of air to the culture to a dissolved-oxygen concentration of 8.4%. The length of the *nox* promoter region in the constructs tested did not dramatically affect CAT activity. Growth with addition of exogenous oxygen to 8.4% resulted in a significant increase in CAT activity in both the 119-bp and the 516-bp *nox* promoter-containing constructs compared to activity derived

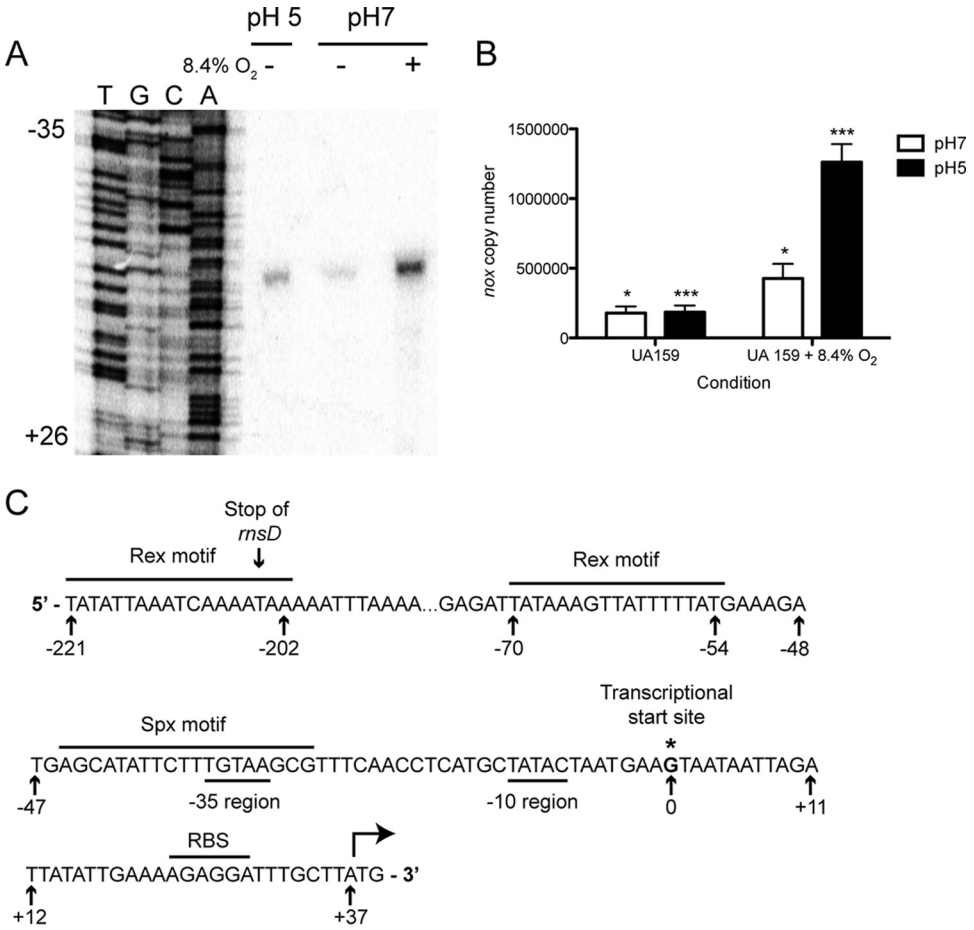

FIG 2 Characterization of the *nox* promoter. (A) Primer extension assay for the identification of the *nox* transcriptional start site. Total RNA was isolated from steady-state cultures of *S. mutans* UA159 grown at pH values of 7 and 5 and with or without the addition of exogenous oxygen (maintained at 8.4%). Lanes with cDNA resulting from the extension of mRNA are indicated as pH 5, pH 7, or pH 7 plus 8.4% O_2. The primer was located at positions +72 to +94 bp in the *nox* open reading frame and was also used to generate the nucleotide ladder. (B) qRT-PCR enumerating *nox* transcripts. RNA from UA159 cells grown to steady state at pH 7 or pH 5 in a chemostat, with or without the addition of 8.4% oxygen. *, statistical significance between pairs, using Student's *t* test, with a *P* value of <0.05 ($n = 12$); ***, statistical significance between pairs, using Student's *t* test, with a *P* value of <0.0001 ($n = 12$). The error bars indicate standard deviations. (C) Nucleotide sequence of the intergenic region preceding *nox*. The site of transcription initiation (asterisk), site of translational initiation (bent arrow), ribosomal binding site (RBS), −10 region, −35 region, conserved Spx and Rex motifs, and end of *rnsD* (SMU.1021) are indicated.

from the respective strains grown without addition of exogenous oxygen (Fig. 3). The results suggest that the mechanism for regulation by oxygen is within the first 119 bp. This is coincident with the location of the predicted Spx regulatory motif, as well as the more proximal Rex regulatory motif.

SpxA affects transcription of *nox*. Microarray and qRT-PCR data have shown previously in *S. mutans* that *nox* transcription is significantly reduced in strains lacking *spxA*, suggesting that the protein promotes *nox* transcription (32). To further examine and confirm the direct influence of Spx proteins on transcription of NADH oxidase, the 119-bp *nox*-CAT reporter construct was integrated into the Δ*spxA*, Δ*spxB*, and Δ*spxAB* strains (32, 37), and samples were harvested from mid-log-phase batch cultures. As expected, *nox* transcription was almost abolished in the Δ*spxA* and Δ*spxAB* strains (Fig. 4A). Interestingly, *nox* transcription was slightly elevated in the Δ*spxB* strain. The results of the CAT reporter assays were confirmed by qRT-PCR performed on RNA extracted from cultures of UA159 or the Δ*spxA* or Δ*spxB* strain grown at pH 7 in continuous culture (Fig. 4B). Highly attenuated growth in chemostat culture prevented measurements using the

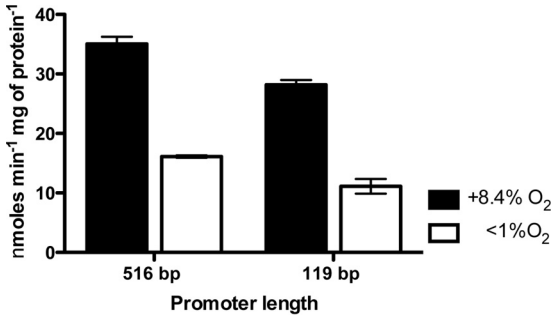

FIG 3 Transcriptional activity of the *nox* promoter. CAT activity was measured using cell extracts of strains grown in batch cultures in a fermentor vessel with or without the addition of exogenous oxygen to 8.4%. The strains contained either 516 bp or 119 bp upstream of *nox* in front of the CAT gene in a UA159 background, as detailed in Materials and Methods. All pairs were found to be statistically significant using Student's *t* test with a *P* value of <0.05 ($n = 3$). The error bars indicate standard deviations.

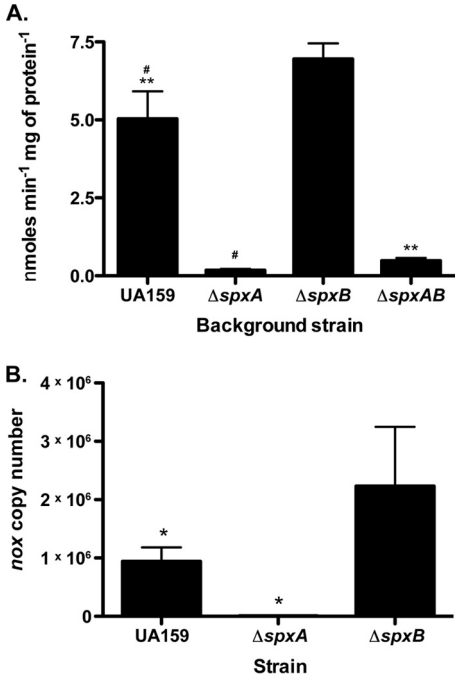

FIG 4 *nox* promoter activity in Δ*spx* strains of *S. mutans*. (A) Chloramphenicol acetyltransferase activity was measured using cell extracts of strains grown in batch culture. Transcription from the 119-bp promoter region preceding *nox* was determined in the following background strains: UA159, Δ*spxA* (JL13), Δ*spxB* (JL12), and Δ*spxAB* (JL21). #, statistical significance between pairs, using Student's *t* test, with a *P* value of <0.05 ($n = 3$); **, statistical significance between pairs, using Student's *t* test, with a *P* value of <0.01 ($n = 3$). The error bars indicate standard deviations. (B) qRT-PCR enumerating *nox* transcripts in RNA extracted from UA159 or the Δ*spxA* or Δ*spxB* strain grown to steady state in a continuous culture. *, statistical significance between pairs, using Student's *t* test, with a *P* value of <0.05 ($n = 3$). The error bars indicate standard deviations.

spxAB double mutant (J. K. Kajfasz and J. A. Lemos, unpublished data). The microarray and CAT reporter assay data strongly suggested that the SpxA protein influences the transcription of RNA message from the promoter region of the *nox* gene. To confirm whether the effects of Spx on *nox* transcription were direct or indirect, IVT assays, using purified SpxA or SpxB protein, were performed. When the *nox* promoter region was incubated with SpxA, a nucleotide transcript was detected that was not present in the absence of SpxA (Fig. 5). When the reaction was repeated in the presence of DTT, the transcript was no longer detected, indicating that SpxA has a positive influence upon the transcription of *nox* but that an oxidizing atmosphere is required for SpxA to exert this effect. When the reaction was repeated with SpxB in place of SpxA, the transcript was not produced, indicating that this regulatory role is specific to SpxA.

Rex directly affects transcription of *nox*. To further confirm the microarray data suggesting that the deletion of *nox* results in an increase in *rex* transcription (Table 5), qRT-PCR was performed to quantify the *rex* transcript in wild-type UA159 cultures grown to steady state at pH 7, with or without addition of oxygen to 8.4%, or in Δ*nox* cultures grown to steady-state at pH 7. Deletion of *nox* resulted in a nearly 3-fold increase in transcription of *rex* (Fig. 6A), confirming the microarray data and suggesting that *nox* may regulate *rex*, perhaps by disrupting the cellular NAD^+/NADH ratios. To assess whether Rex regulates *nox* transcription,

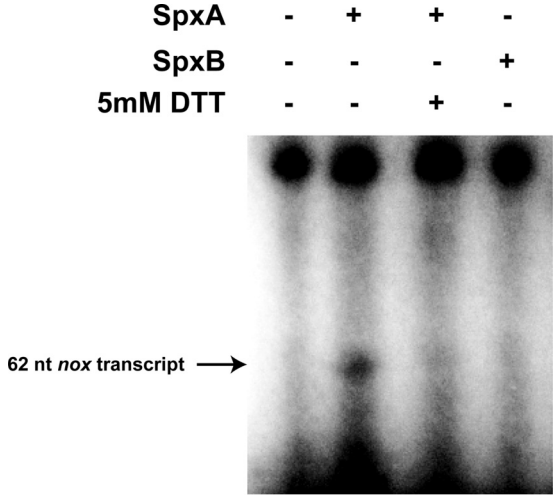

FIG 5 SpxA promotes *in vitro* transcription of *nox*. The *nox* promoter was incubated with *B. subtilis* RNAP and *B. subtilis* σ^A with or without SpxA or SpxB protein and DTT.

the 119-bp and 516-bp *nox*-CAT constructs were transformed into the Δ*rex* mutant strain, generating strains Δ*rex*-P*nox*119 (UR322) and Δ*rex*-P*nox*516 (UR323) (Table 1). A CAT activity assay was performed to compare Δ*rex*-P*nox*119 (UR322) and

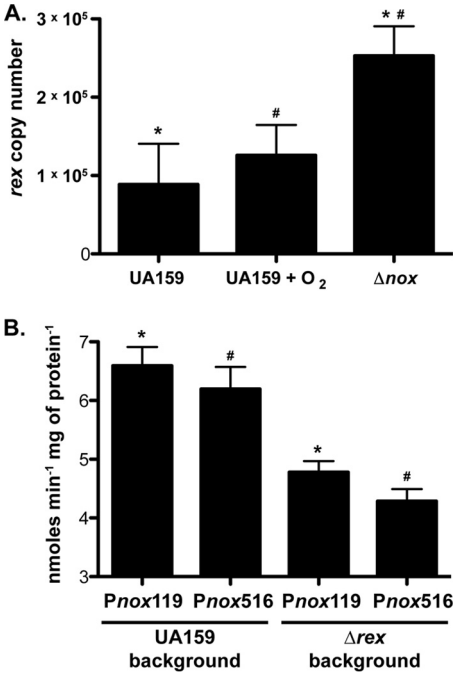

FIG 6 Inverse relationship of *rex* and *nox* transcript levels. (A) qRT-PCR enumerating *rex* transcripts in RNA extracted from UA159, UA159 plus 8.4% O_2, and Δ*nox* strains grown to steady state at pH 7 in continuous culture. * and #, statistical significance between pairs, using Student's *t* test, with a *P* value of <0.05 ($n = 5$). The error bars indicate standard deviations. (B) *nox* promoter activity was quantified by CAT activity measurements as described in Materials and Methods, using cell extracts of strains grown in batch culture. Transcription from the 119-bp and 516-bp promoter regions preceding *nox* was determined in UA159 (parent strain) and Δ*rex* backgrounds. * and #, statistical significance between pairs, using Student's *t* test, with a *P* value of <0.0001 ($n = 5$). The error bars indicate standard deviations.

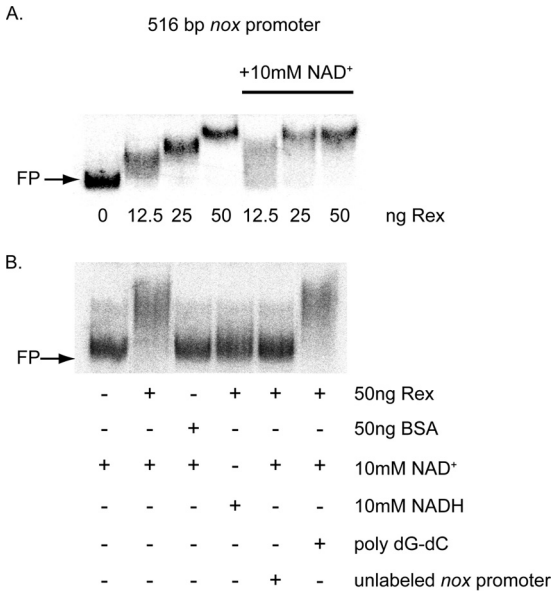

FIG 7 Rex binds to the *nox* promoter. (A) Electrophoretic mobility shift assays were performed with radiolabeled *nox* promoter probe incubated with the indicated amount of purified Rex protein with or without the addition of 10 mM NAD^+. The arrow at the left indicates migration of the free probe (FP). (B) An electrophoretic mobility shift assay was also performed to demonstrate specificity of the binding reaction. FP, indicated by the arrow, was incubated in the presence of 50 ng Rex with 10 mM NAD^+, 10 mM NADH, and 10 mM NAD^+ plus unlabeled cognate competitor (80 ng, or 200 times the labeled probe) or 10 mM NAD^+ plus 2 ng poly(dG-dC). A control reaction was also performed with BSA plus 10 mM NAD^+.

Δ*rex*-P*nox*516 (UR323) to UA159-P*nox*119 (UR130) and UA159-P*nox*516 (UR281), the 119-bp and 516-bp *nox*-CAT reporter constructs in the parental UA159 background, respectively. The CAT activity was significantly reduced in the Δ*rex* background for both promoter length constructs compared to their counterparts in the UA159 background (Fig. 6B), further supporting a model of Rex acting as a positive regulator of *nox*. Finally, an EMSA was performed to show that the Rex protein specifically bound to the *nox* promoter. Indeed, when the 516-bp *nox* promoter was labeled with ^{32}P and incubated with increasing amounts of Rex protein, increases in the shifted DNA-protein complex were also observed (Fig. 7). The mobility of the complex was slightly improved upon addition of 10 mM NAD^+, shown previously to be a cofactor in Rex binding (38). A shift in the labeled DNA was not seen upon addition of 10 mM NADH, previously shown to inhibit binding of Rex to target promoters (38) (Fig. 7B). Competition with excess unlabeled probe or a binding reaction with BSA as a negative control demonstrated specificity of the Rex-*nox* binding reaction (Fig. 7B). Addition of unlabeled excess poly(dG-dC) to the reaction mixture led to a mobility shift of the complex similar to that observed without addition of poly(dG-dC) (Fig. 7B). Collectively, these data show that Rex binds specifically to the *nox* promoter and enhances *nox* transcription, which is inhibited by NADH.

DISCUSSION

Exposure to oxygen and loss of *nox* lead to global changes in the *S. mutans* transcriptome. As both a reducer of oxygen and a regenerator of NAD^+, Nox plays an important role in affecting the levels of both of these cellular metabolites, which have been shown to influence global regulatory pathways (21, 31, 34, 38, 64). We therefore wanted to observe the effects of the loss of *nox* on the *S. mutans* transcriptome. The results of this study indicate that the transcriptional profile of genes differentially expressed in the wild-type strain upon addition of exogenous oxygen bears many similarities to the transcriptional profile of genes differentially expressed in the Δ*nox* strain. In fact, 85 genes were differentially regulated under both conditions compared to UA159 without addition of exogenous oxygen. These similarities include altered expression of genes encoding proteins involved in energy metabolism, transport and binding, and detoxification (Fig. 1). More specifically, upregulation of genes participating in alleviation of ROS stress and downregulation of genes encoding several key enzymes in sugar metabolism pathways were observed (Tables 4 and 5). These findings are plausible, as the most logical targets of upregulation during oxidative stress are the enzymes used to reduce and eliminate oxygen and deleterious ROS, such as *nox*, *gor*, *sod*, *trxA*, *ahpCF*, *tpx*, and *dpr*. It has been reported previously that *S. mutans* produces elevated levels of acetoin under aerobic conditions (65). Therefore, it is unsurprising that our microarray data showed elevated transcription of acetoin dehydrogenase genes under conditions of oxidative stress, as the enzyme complex would be necessary to metabolize the larger amount of acetoin produced under these circumstances (Table 5).

Although there was a great deal of similarity in the array and qRT-PCR data derived from UA159 plus 8.4% O_2 and the Δ*nox* strain, there were several differences, indicating that the effects of the loss of *nox* are not limited to those stemming from exposure to additional oxygen. Fifteen more genes known to encode proteins involved in signal transduction were upregulated in the Δ*nox* strain than in UA159 plus 8.4% O_2. An additional 11 known transcription factors were upregulated in the Δ*nox* strain but not in UA159 plus 8.4% O_2. One possibility is that these differences were due to perturbed NAD^+/NADH levels due to the loss of *nox*. It is highly likely that redox-sensing proteins, rather than the Nox protein directly, serve to upregulate the ROS-metabolizing enzymes during times of high oxygen tension. Indeed, the redox-sensing regulator Rex was upregulated in the the Δ*nox* strain microarray but not in the UA159-plus-8.4% O_2 microarray. This is likely due to the fact that Rex binds to its own promoter in an inhibitory fashion when bound to NAD^+ (38). Deletion of *nox* may impair regeneration of NAD^+, and low NAD^+ levels would lead to dissociation of Rex from target promoters, including its own. In addition to Rex, Spx proteins are regulators modulated by oxygen levels, and it has been shown previously that Gor and Sod activity, in addition to Nox activity, are coupled to the *S. mutans* Spx regulatory network (32).

Regulation of *nox* in *S. mutans*. The majority of the research devoted to regulation of *nox* in Gram-positive bacteria has been in organisms used in the food industry. Both *Lactococcus lactis* and *Lactobacillus sanfranciscensis* have demonstrated regulation of NADH oxidase by oxygen; thus, it is plausible that *nox* in *S. mutans* is similarly regulated (66, 67). Previous research had identified the Spx protein(s) as a regulator of oxygen homeostasis in both *B. subtilis* and *S. mutans* (32, 64, 68). In *B. subtilis*, Spx regulation is controlled by the redox state, with oxidation of a CXXC motif at the N terminus activating the protein and facilitating its interaction with the C-terminal domain of the RNAP (34, 64). Thus, *B. subtilis* Spx senses oxygen levels and adjusts appropriate downstream transcription levels accordingly. Although the exact

mechanism for SpxA activation in *S. mutans* is unknown, the data described in this study further demonstrate the activation of *nox* transcription by the Spx homolog, SpxA, in *S. mutans*. The proximal 119 bp upstream of the *nox* translational start site is sufficient for oxygen-mediated control of *nox* transcription (Fig. 3). The sequence in the −35 to −42 region resembles the motif found to be important for Spx activation of the *trx* gene in *B. subtilis*, although the *S. mutans* region contains an additional 4 or 5 bp (Fig. 2C). The extended sequence would most likely interact with the αCTD of the RNA polymerase, and it is possible that the *S. mutans* αCTD has different conformational folding or is slightly larger than that found in *B. subtilis*. The data described above suggest that SpxA in *S. mutans* behaves in an oxygen-sensing regulatory manner similar to that of the *B. subtilis* Spx. Indeed, both SpxA and SpxB in *S. mutans* contain the regulatory CXXC motif seen in the *B. subtilis* Spx (32) and likely bind to and regulate target sequences such as the *nox* promoter when in the oxidized state. Indeed, an *in vitro* transcription assay of the *nox* promoter showed transcript generated in the presence of SpxA that was not generated in its absence. Additionally, the transcript was not generated in the presence of SpxA when DTT was added to the reaction mixture, indicating that SpxA does not promote *nox* transcription while in a reducing environment (Fig. 5). Thus, it appears that exposure to an elevated oxygen concentration and/or the loss of *nox* impacts the organism through the regulator SpxA. It is reasonable to propose that the oxidized form of SpxA is then able to regulate the transcription of *nox* and other oxidative-stress genes, such as *gor*, *sod*, *tpx*, and *trx*, through interaction with the RNA polymerase. Indeed, qRT-PCR and CAT assay data showed that SpxA affects *nox* transcription (Fig. 4). Since SpxB did not produce a *nox* transcript (Fig. 5) and did not exert any statistically significant changes in *nox* transcription (Fig. 4), it appears unlikely that it plays a role in regulation of *nox*. It is likely that changes in the expression of the aforementioned oxidative-stress genes may also impact other pathways, such as energy metabolism and membrane and cell wall homeostasis. In fact, it has been previously demonstrated that there is an elevation in unsaturated fatty acid production in cells grown under elevated oxygen tension (21). It is conceivable, then, that some of the changes we see in the Δ*nox* microarrays are a result of increased activity of Spx, due to increased oxygen tension, rather than a direct effect of the loss of *nox*. An example of this is the apparent upregulation of *adhABCD*, encoding acetoin dehydrogenase, both in the Δ*nox* mutant and in UA159 grown with 8.4% O_2 (Table 5). The *adhABCD* cluster has been shown previously to be downregulated in the *spxA* mutant, suggesting that SpxA positively regulates these genes (32). Direct addition of oxygen, or loss of *nox*, would favor oxidation of SpxA, making it more active, allowing upregulation of *adhABCD*.

In this study, *in silico* analysis identified two putative Rex-binding sites in the *nox* promoter. It has been shown previously that Rex activity is regulated by NAD^+/NADH levels and has modulatory effects on a variety of processes, including carbon metabolism, acid and oxygen stress responses, and biofilm formation (31, 38). Rex binds to target DNA and exerts its regulatory effects when bound to NAD^+, but not when bound to NADH (31, 38). It has been previously suggested by qRT-PCR data that *nox* may be a target for Rex regulation (31, 38). As stated above, *nox* appears to regulate *rex*, and thus, *rex* and *nox* may be involved in a regulatory loop where Nox affects NAD^+ levels, which affect Rex DNA-binding activity and expression through autoregulation, and Rex binds

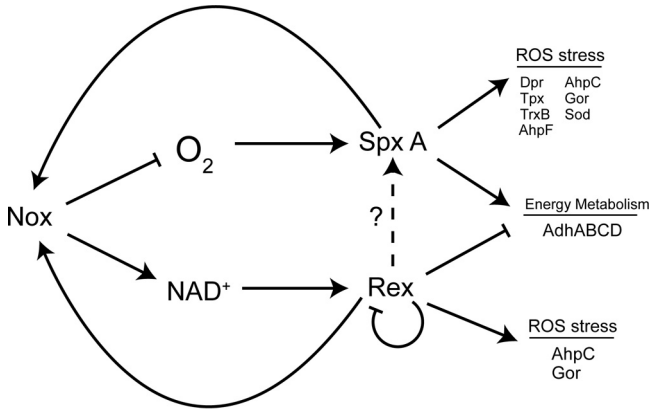

FIG 8 Proposed model for the role of Nox in the Spx and Rex regulons. Nox generates NAD^+, which, when bound, activates the transcriptional-regulatory activity of Rex. Rex positively regulates the ROS stress genes *nox*, *ahpC*, and *gor* while downregulating itself and *adhABCD*. Rex may also regulate *spxA* (dashed line). Nox metabolizes oxygen, which, when abundant, leads to oxidation of SpxA, activating its transcriptional-regulatory activity. When active, SpxA positively regulates the ROS stress genes *nox*, *dpr*, *tpx*, *trxB*, *ahpCF*, *gor*, and *sod*, as well as the *adhABCD* complex.

to the *nox* promoter and regulates *nox*. Indeed, EMSA analysis showed that Rex bound specifically to the promoter region of *nox* (Fig. 7), and CAT reporter data strongly suggested that Rex acts as a positive regulator of *nox* (Fig. 6B). This regulatory loop is reminiscent of the Rex and NADH oxidase regulatory loop identified previously in *B. subtilis* (69). Interestingly, we also found a Rex-binding motif in the promoter region of *spxA* (data not shown), although further work is required to determine whether Rex regulates *spxA*. Deletion of *nox* would decouple the SpxA regulon from the Rex regulon, as oxygen levels and NAD^+ levels lose their most direct link. As Rex is a positive regulator of oxidative-stress genes, including *nox*, *gor*, and *ahpC* (31, 38), their apparent upregulation in the absence of *nox* is likely due to SpxA and not Rex, as Rex is likely in its NADH-bound, inactive state. Rex negatively regulates the acetoin dehydrogenase pathway (31, 38), and therefore, it is unclear whether the upregulation seen in the associated genes in our microarrays is due to oxygen-induced SpxA activation, inactivation of Rex, or both. A potential regulatory network is depicted in Fig. 8, where Nox is a central player, fine-tuning oxygen and NAD^+ levels, which in turn are sensed by SpxA and Rex, respectively, driving modulation of their regulons.

Conclusions. From the present study, we conclude that the NADH oxidase enzyme lies at the intersection of multiple regulatory pathways (Fig. 8) and is itself regulated by these pathways. Through its role in reducing oxygen, Nox could negatively modulate the activity of SpxA, which has multiple downstream targets. Additionally, through generation of NAD^+, Nox regulates Rex, which, like SpxA, has a large and diverse regulon, including many genes involved in acid and oxidative stress, transport, energy metabolism, and biofilm formation—functions critical to persistence of the oral pathogen *S. mutans*. Studies are in progress to further clarify the relationships between the Spx proteins, *nox*, Rex, and NAD^+/NADH ratios and to expand our knowledge of the associated regulatory networks.

ACKNOWLEDGMENTS

This study was supported by the Training Program in Oral Sciences, NIH/NIDCR T32 DE-07165 (A.M.D.) and T90-DE021985 (J.L.B.), and by

NIH/NIDCR DE-13683 (R.G.Q.), NIH/NIDCR DE-17425 (R.G.Q.), NIH/NIDCR DE-19452 (Z.T.W.), and NIH/NIDCR DE-019783 (J.A.L.).

We thank Jeremiah Baldeck for his assistance. We also thank Peter Zuber for the gifts of *B. subtilis* RNAP and σ^A.

REFERENCES

1. **Koo H, Xiao J, Klein MI, Jeon JG.** 2010. Exopolysaccharides produced by *Streptococcus mutans* glucosyltransferases modulate the establishment of microcolonies within multispecies biofilms. J. Bacteriol. **192:**3024–3032. http://dx.doi.org/10.1128/JB.01649-09.
2. **Marsh PD.** 2004. Dental plaque as a microbial biofilm. Caries Res. **38:**204–211. http://dx.doi.org/10.1159/000077756.
3. **Xiao J, Koo H.** 2010. Structural organization and dynamics of exopolysaccharide matrix and microcolonies formation by *Streptococcus mutans* in biofilms. J. Appl. Microbiol. **108:**2103–2113. http://dx.doi.org/10.1111/j.1365-2672.2009.04616.x.
4. **Lemos JA, Quivey RG, Jr, Koo H, Abranches J.** 2013. *Streptococcus mutans*: a new Gram-positive paradigm? Microbiology **159:**436–445. http://dx.doi.org/10.1099/mic.0.066134-0.
5. **Lemos JA, Burne RA.** 2008. A model of efficiency: stress tolerance by *Streptococcus mutans*. Microbiology **154:**3247–3255. http://dx.doi.org/10.1099/mic.0.2008/023770-0.
6. **Bowden GH, Hamilton IR.** 1998. Survival of oral bacteria. Crit. Rev. Oral Biol. Med. **9:**54–85. http://dx.doi.org/10.1177/10454411980090010401.
7. **Kuhnert WL, Quivey RG, Jr.** 2003. Genetic and biochemical characterization of the F-ATPase operon from *Streptococcus sanguis* 10904. J. Bacteriol. **185:**1525–1533. http://dx.doi.org/10.1128/JB.185.5.1525-1533.2003.
8. **Sheng J, Marquis RE.** 2006. Enhanced acid resistance of oral streptococci at lethal pH values associated with acid-tolerant catabolism and with ATP synthase activity. FEMS Microbiol. Lett. **262:**93–98. http://dx.doi.org/10.1111/j.1574-6968.2006.00374.x.
9. **Abranches J, Candella MM, Wen ZT, Baker HV, Burne RA.** 2006. Different roles of $EIIAB^{Man}$ and EII^{Glc} in regulation of energy metabolism, biofilm development, and competence in *Streptococcus mutans*. J. Bacteriol. **188:**3748–3756. http://dx.doi.org/10.1128/JB.00169-06.
10. **Abranches J, Nascimento MM, Zeng L, Browngardt CM, Wen ZT, Rivera MF, Burne RA.** 2008. CcpA regulates central metabolism and virulence gene expression in *Streptococcus mutans*. J. Bacteriol. **190:**2340–2349. http://dx.doi.org/10.1128/JB.01237-07.
11. **Griswold AR, Jameson-Lee M, Burne RA.** 2006. Regulation and physiologic significance of the agmatine deiminase system of *Streptococcus mutans* UA159. J. Bacteriol. **188:**834–841. http://dx.doi.org/10.1128/JB.188.3.834-841.2006.
12. **Sheng J, Marquis RE.** 2007. Malolactic fermentation by *Streptococcus mutans*. FEMS Microbiol. Lett. **272:**196–201. http://dx.doi.org/10.1111/j.1574-6968.2007.00744.x.
13. **Fozo EM, Quivey RG, Jr.** 2004. Shifts in the membrane fatty acid profile of *Streptococcus mutans* enhance survival in acidic environments. Appl. Environ. Microbiol. **70:**929–936. http://dx.doi.org/10.1128/AEM.70.2.929-936.2004.
14. **Fozo EM, Scott-Anne K, Koo H, Quivey RG, Jr.** 2007. Role of unsaturated fatty acid biosynthesis in virulence of *Streptococcus mutans*. Infect. Immun. **75:**1537–1539. http://dx.doi.org/10.1128/IAI.01938-06.
15. **Liu L, Tong H, Dong X.** 2012. Function of the pyruvate oxidase-lactate oxidase cascade in interspecies competition between *Streptococcus oligofermentans* and *Streptococcus mutans*. Appl. Environ. Microbiol. **78:**2120–2127. http://dx.doi.org/10.1128/AEM.07539-11.
16. **Zheng LY, Itzek A, Chen ZY, Kreth J.** 2011. Oxygen dependent pyruvate oxidase expression and production in *Streptococcus sanguinis*. Int. J. Oral Sci. **3:**82–89. http://dx.doi.org/10.4248/IJOS11030.
17. **Kreth J, Merritt J, Shi W, Qi F.** 2005. Competition and coexistence between *Streptococcus mutans* and *Streptococcus sanguinis* in the dental biofilm. J. Bacteriol. **187:**7193–7203. http://dx.doi.org/10.1128/JB.187.21.7193-7203.2005.
18. **Ryan CS, Kleinberg I.** 1995. Bacteria in human mouths involved in the production and utilization of hydrogen peroxide. Arch. Oral Biol. **40:**753–763. http://dx.doi.org/10.1016/0003-9969(95)00029-O.
19. **Tong H, Chen W, Merritt J, Qi F, Shi W, Dong X.** 2007. *Streptococcus oligofermentans* inhibits *Streptococcus mutans* through conversion of lactic acid into inhibitory H_2O_2: a possible counteroffensive strategy for interspecies competition. Mol. Microbiol. **63:**872–880. http://dx.doi.org/10.1111/j.1365-2958.2006.05546.x.
20. **Ajdic D, McShan WM, McLaughlin RE, Savic G, Chang J, Carson MB, Primeaux C, Tian R, Kenton S, Jia H, Lin S, Qian Y, Li S, Zhu H, Najar F, Lai H, White J, Roe BA, Ferretti JJ.** 2002. Genome sequence of *Streptococcus mutans* UA159, a cariogenic dental pathogen. Proc. Natl. Acad. Sci. U. S. A. **99:**14434–14439. http://dx.doi.org/10.1073/pnas.172501299.
21. **Derr AM, Faustoferri RC, Betzenhauser MJ, Gonzalez K, Marquis RE, Quivey RG, Jr.** 2012. Mutation of the NADH oxidase gene (*nox*) reveals an overlap of the oxygen- and acid-mediated stress responses in *Streptococcus mutans*. Appl. Environ. Microbiol. **78:**1215–1227. http://dx.doi.org/10.1128/AEM.06890-11.
22. **Higuchi T, Imamura Y, Otagiri M.** 1993. Kinetic studies on the reduction of acetohexamide catalyzed by carbonyl reductase from rabbit kidney. Biochim. Biophys. Acta **1158:**23–28. http://dx.doi.org/10.1016/0304-4165(93)90091-L.
23. **Higuchi M, Yamamoto Y, Poole LB, Shimada M, Sato Y, Takahashi N, Kamio Y.** 1999. Functions of two types of NADH oxidases in energy metabolism and oxidative stress of *Streptococcus mutans*. J. Bacteriol. **181:**5940–5947.
24. **Pesakhov S, Benisty R, Sikron N, Cohen Z, Gomelsky P, Khozin-Goldberg I, Dagan R, Porat N.** 2007. Effect of hydrogen peroxide production and the Fenton reaction on membrane composition of *Streptococcus pneumoniae*. Biochim. Biophys. Acta **1768:**590–597. http://dx.doi.org/10.1016/j.bbamem.2006.12.016.
25. **Yamamoto Y, Pargade V, Lamberet G, Gaudu P, Thomas F, Texereau J, Gruss A, Trieu-Cuot P, Poyart C.** 2006. The Group B Streptococcus NADH oxidase Nox-2 is involved in fatty acid biosynthesis during aerobic growth and contributes to virulence. Mol. Microbiol. **62:**772–785. http://dx.doi.org/10.1111/j.1365-2958.2006.05406.x.
26. **Abbe K, Carlsson J, Takahashi-Abbe S, Yamada T.** 1991. Oxygen and the sugar metabolism in oral streptococci. Proc. Finn. Dent. Soc. **87:**477–487.
27. **Carlsson J, Griffith CJ.** 1974. Fermentation products and bacterial yields in glucose-limited and nitrogen-limited cultures of streptococci. Arch. Oral Biol. **19:**1105–1109. http://dx.doi.org/10.1016/0003-9969(74)90238-6.
28. **Yamada T, Carlsson J.** 1975. Regulation of lactate dehydrogenase and change of fermentation products in streptococci. J. Bacteriol. **124:**55–61.
29. **Smith EG, Spatafora GA.** 2012. Gene regulation in *S. mutans*: complex control in a complex environment. J. Dent. Res. **91:**133–141. http://dx.doi.org/10.1177/0022034511415415.
30. **Higuchi M, Yamamoto Y, Kamio Y.** 2000. Molecular biology of oxygen tolerance in lactic acid bacteria: functions of NADH oxidases and Dpr in oxidative stress. J. Biosci. Bioeng. **90:**484–493. http://dx.doi.org/10.1016/S1389-1723(01)80028-1.
31. **Bitoun JP, Nguyen AH, Fan Y, Burne RA, Wen ZT.** 2011. Transcriptional repressor Rex is involved in regulation of oxidative stress response and biofilm formation by *Streptococcus mutans*. FEMS Microbiol. Lett. **320:**110–117. http://dx.doi.org/10.1111/j.1574-6968.2011.02293.x.
32. **Kajfasz JK, Rivera-Ramos I, Abranches J, Martinez AR, Rosalen PL, Derr AM, Quivey RG, Lemos JA.** 2010. Two Spx proteins modulate stress tolerance, survival, and virulence in *Streptococcus mutans*. J. Bacteriol. **192:**2546–2556. http://dx.doi.org/10.1128/JB.00028-10.
33. **Lin AA, Walthers D, Zuber P.** 2013. Residue substitutions near the redox center of *Bacillus subtilis* Spx affect RNA polymerase interaction, redox control, and Spx-DNA contact at a conserved cis-acting element. J. Bacteriol. **195:**3967–3978. http://dx.doi.org/10.1128/JB.00645-13.
34. **Nakano S, Erwin KN, Ralle M, Zuber P.** 2005. Redox-sensitive transcriptional control by a thiol/disulphide switch in the global regulator, Spx. Mol. Microbiol. **55:**498–510. http://dx.doi.org/10.1111/j.1365-2958.2004.04395.x.
35. **Nakano S, Nakano MM, Zhang Y, Leelakriangsak M, Zuber P.** 2003. A regulatory protein that interferes with activator-stimulated transcription in bacteria. Proc. Natl. Acad. Sci. U. S. A. **100:**4233–4238. http://dx.doi.org/10.1073/pnas.0637648100.
36. **Reyes DY, Zuber P.** 2008. Activation of transcription initiation by Spx: formation of transcription complex and identification of a cis-acting element required for transcriptional activation. Mol. Microbiol. **69:**765–779. http://dx.doi.org/10.1111/j.1365-2958.2008.06330.x.
37. **Kajfasz JK, Martinez AR, Rivera-Ramos I, Abranches J, Koo H, Quivey RG, Jr, Lemos JA.** 2009. Role of Clp proteins in expression of virulence properties of *Streptococcus mutans*. J. Bacteriol. **191:**2060–2068. http://dx.doi.org/10.1128/JB.01609-08.
38. **Bitoun JP, Liao S, Yao X, Xie GG, Wen ZT.** 2012. The redox-sensing regulator Rex modulates central carbon metabolism, stress tolerance re-

sponse and biofilm formation by *Streptococcus mutans*. PLoS One **7:**e44766. http://dx.doi.org/10.1371/journal.pone.0044766.
39. **Ravcheev DA, Li X, Latif H, Zengler K, Leyn SA, Korostelev YD, Kazakov AE, Novichkov PS, Osterman AL, Rodionov DA.** 2012. Transcriptional regulation of central carbon and energy metabolism in bacteria by redox-responsive repressor Rex. J. Bacteriol. **194:**1145–1157. http://dx.doi.org/10.1128/JB.06412-11.
40. **Pagels M, Fuchs S, Pane-Farre J, Kohler C, Menschner L, Hecker M, McNamarra PJ, Bauer MC, von Wachenfeldt C, Liebeke M, Lalk M, Sander G, von Eiff C, Proctor RA, Engelmann S.** 2010. Redox sensing by a Rex-family repressor is involved in the regulation of anaerobic gene expression in *Staphylococcus aureus*. Mol. Microbiol. **76:**1142–1161. http://dx.doi.org/10.1111/j.1365-2958.2010.07105.x.
41. **Brekasis D, Paget MS.** 2003. A novel sensor of NADH/NAD+ redox poise in *Streptomyces coelicolor* A3(2). EMBO J. **22:**4856–4865. http://dx.doi.org/10.1093/emboj/cdg453.
42. **Wang E, Bauer MC, Rogstam A, Linse S, Logan DT, von Wachenfeldt C.** 2008. Structure and functional properties of the *Bacillus subtilis* transcriptional repressor Rex. Mol. Microbiol. **69:**466–478. http://dx.doi.org/10.1111/j.1365-2958.2008.06295.x.
43. **McLaughlin KJ, Strain-Damerell CM, Xie K, Brekasis D, Soares AS, Paget MS, Kielkopf CL.** 2010. Structural basis for NADH/NAD+ redox sensing by a Rex family repressor. Mol. Cell **38:**563–575. http://dx.doi.org/10.1016/j.molcel.2010.05.006.
44. **Murchison HH, Barrett JF, Cardineau GA, Curtiss R, III.** 1986. Transformation of *Streptococcus mutans* with chromosomal and shuttle plasmid (pYA629) DNAs. Infect. Immun. **54:**273–282.
45. **Quivey RG, Jr, Faustoferri RC, Clancy KA, Marquis RE.** 1995. Acid adaptation in *Streptococcus mutans* UA159 alleviates sensitization to environmental stress due to RecA deficiency. FEMS Microbiol. Lett. **126:**257–261. http://dx.doi.org/10.1111/j.1574-6968.1995.tb07427.x.
46. **Quivey RG, Jr, Faustoferri RC, Belli WA, Flores JS.** 1991. Polymerase chain reaction amplification, cloning, sequence determination and homologies of streptococcal ATPase-encoding DNAs. Gene **97:**63–68. http://dx.doi.org/10.1016/0378-1119(91)90010-9.
47. **Perry D, Kuramitsu HK.** 1981. Genetic transformation of *Streptococcus mutans*. Infect. Immun. **32:**1295–1297.
48. **Aslanidis C, de Jong PJ.** 1990. Ligation-independent cloning of PCR products (LIC-PCR). Nucleic Acids Res. **18:**6069–6074. http://dx.doi.org/10.1093/nar/18.20.6069.
49. **Lau PC, Sung CK, Lee JH, Morrison DA, Cvitkovitch DG.** 2002. PCR ligation mutagenesis in transformable streptococci: application and efficiency. J. Microbiol. Methods **49:**193–205. http://dx.doi.org/10.1016/S0167-7012(01)00369-4.
50. **Sheng J, Baldeck JD, Nguyen PT, Quivey RG, Jr, Marquis RE.** 2010. Alkali production associated with malolactic fermentation by oral streptococci and protection against acid, oxidative, or starvation damage. Can. J. Microbiol. **56:**539–547. http://dx.doi.org/10.1139/W10-039.
51. **Wen ZT, Burne RA.** 2001. Construction of a new integration vector for use in *Streptococcus mutans*. Plasmid **45:**31–36. http://dx.doi.org/10.1006/plas.2000.1498.
52. **Kuhnert WL, Zheng G, Faustoferri RC, Quivey RG, Jr.** 2004. The F-ATPase operon promoter of *Streptococcus mutans* is transcriptionally regulated in response to external pH. J. Bacteriol. **186:**8524–8528. http://dx.doi.org/10.1128/JB.186.24.8524-8528.2004.
53. **Shaw WV.** 1975. Chloramphenicol acetyltransferase from chloramphenicol-resistant bacteria. Methods Enzymol. **43:**737–755. http://dx.doi.org/10.1016/0076-6879(75)43141-X.
54. **Abranches J, Miller JH, Martinez AR, Simpson-Haidaris PJ, Burne RA, Lemos JA.** 2011. The collagen-binding protein Cnm is required for *Streptococcus mutans* adherence to and intracellular invasion of human coronary artery endothelial cells. Infect. Immun. **79:**2277–2284. http://dx.doi.org/10.1128/IAI.00767-10.
55. **Smith AJ, Quivey RG, Jr, Faustoferri RC.** 1996. Cloning and nucleotide sequence analysis of the *Streptococcus mutans* membrane-bound, proton-translocating ATPase operon. Gene **183:**87–96. http://dx.doi.org/10.1016/S0378-1119(96)00502-1.
56. **Smith PK, Krohn RI, Hermanson GT, Mallia AK, Gartner FH, Provenzano MD, Fujimoto EK, Goeke NM, Olson BJ, Klenk DC.** 1985. Measurement of protein using bicinchoninic acid. Anal. Biochem. **150:**76–85. http://dx.doi.org/10.1016/0003-2697(85)90442-7.
57. **Lin AA, Zuber P.** 2012. Evidence that a single monomer of Spx can productively interact with RNA polymerase in *Bacillus subtilis*. J. Bacteriol. **194:**1697–1707. http://dx.doi.org/10.1128/JB.06660-11.
58. **Ahn SJ, Wen ZT, Burne RA.** 2007. Effects of oxygen on virulence traits of *Streptococcus mutans*. J. Bacteriol. **189:**8519–8527. http://dx.doi.org/10.1128/JB.01180-07.
59. **Ahn SJ, Ahn SJ, Browngardt CM, Burne RA.** 2009. Changes in biochemical and phenotypic properties of *Streptococcus mutans* during growth with aeration. Appl. Environ. Microbiol. **75:**2517–2527. http://dx.doi.org/10.1128/AEM.02367-08.
60. **Gong Y, Tian XL, Sutherland T, Sisson G, Mai J, Ling J, Li YH.** 2009. Global transcriptional analysis of acid-inducible genes in *Streptococcus mutans*: multiple two-component systems involved in acid adaptation. Microbiology **155:**3322–3332. http://dx.doi.org/10.1099/mic.0.031591-0.
61. **Yamada T, Kimura S, Igarashi K.** 1980. Metabolism of glucosylsucrose and maltosylsucrose by *Streptococcus mutans*. Caries Res. **14:**139–147.
62. **Iwami Y, Yamada T.** 1980. Rate-limiting steps of the glycolytic pathway in the oral bacteria *Streptococcus mutans* and *Streptococcus sanguis* and the influence of acidic pH on the glucose metabolism. Arch. Oral Biol. **25:**163–169. http://dx.doi.org/10.1016/0003-9969(80)90015-1.
63. **Rice P, Longden I, Bleasby A.** 2000. EMBOSS: the European Molecular Biology Open Software Suite. Trends Genet. **16:**276–277. http://dx.doi.org/10.1016/S0168-9525(00)02024-2.
64. **Nakano MM, Lin A, Zuber CS, Newberry KJ, Brennan RG, Zuber P.** 2010. Promoter recognition by a complex of Spx and the C-terminal domain of the RNA polymerase alpha subunit. PLoS One **5:**e8664. http://dx.doi.org/10.1371/journal.pone.0008664.
65. **Hillman JD, Andrews SW, Dzuback AL.** 1987. Acetoin production by wild-type strains and a lactate dehydrogenase-deficient mutant of *Streptococcus mutans*. Infect. Immun. **55:**1399–1402.
66. **Jansch A, Freiding S, Behr J, Vogel RF.** 2011. Contribution of the NADH-oxidase (Nox) to the aerobic life of *Lactobacillus sanfranciscensis* DSM20451T. Food Microbiol. **28:**29–37. http://dx.doi.org/10.1016/j.fm.2010.08.001.
67. **Lopez de Felipe F, Kleerebezem M, de Vos WM, Hugenholtz J.** 1998. Cofactor engineering: a novel approach to metabolic engineering in *Lactococcus lactis* by controlled expression of NADH oxidase. J. Bacteriol. **180:**3804–3808.
68. **Nakano S, Kuster-Schock E, Grossman AD, Zuber P.** 2003. Spx-dependent global transcriptional control is induced by thiol-specific oxidative stress in *Bacillus subtilis*. Proc. Natl. Acad. Sci. U. S. A. **100:**13603–13608. http://dx.doi.org/10.1073/pnas.2235180100.
69. **Gyan S, Shiohira Y, Sato I, Takeuchi M, Sato T.** 2006. Regulatory loop between redox sensing of the NADH/NAD(+) ratio by Rex (YdiH) and oxidation of NADH by NADH dehydrogenase Ndh in *Bacillus subtilis*. J. Bacteriol. **188:**7062–7071. http://dx.doi.org/10.1128/JB.00601-06.